Nigerian Journal of Physics (NJP)
ISSN online: 3027-0936
ISSN print: 1595-0611
DOI: https://doi.org/10.62292/njp.v33i1.2024.197
Volume 33(1), March 2024

# Geophysical and Sedimentological Characterization of Oil Sand Deposit in Part of Eastern Dahomey Basin Southwestern Nigeria

***Adekoya, S. A., Coker, J. O., Ikhane, P. R. and Oladunjoye, H. T.**

Olabisi Onabanjo University, Ago-Iwoye

*Corresponding author's email: Adekoya.sofiat@oouagoiwoye.edu.ng

**ABSTRACT**

Unconventional oil is the group name given to unconventional petroleum deposits such as oil sands and heavy oils. Oil sand, commonly referred to as tar sand or bituminous sand is a sandstone formation impregnated with viscous bitumen. This study utilized the two-dimensional electrical resistivity imaging technique to characterize oil sand and validate its true resistivity value and sedimentological analysis to evaluate the physical properties of the oil sand deposit. The two-dimension electrical resistivity imaging data acquisition was done along seven profiles systematically in a grid format using dipole-dipole electrode configuration and processed using the RES2DINV software. Fresh samples were collected from three points within the study area for grain sizes and textural properties analysis. The result of the 2-D ERI in the study area showed two to three geoelectric layers and the oil sand being the second layer as evident in the 3-D model obtained from the systemic data acquisition procedure. The resistivity obtained for oil sand in the study area range between 2,500 Ωm to $10^5$ Ωm which validates the report of high resistivity value of oil sand in the study area. The sedimentological analysis showed that the sediments in the study area are of medium sand moderately sorted sand grain and leptokurtic to mesokurtic sand suggesting unimodal and bimodal parent source.

**Keywords:**
Oil sand,
Resistivity,
Sand,
Deposit,
Kurtosis.

## INTRODUCTION

The Nigerian oil sands deposit belt as reported from previous geophysical studies by (Adegoke *et al.,* 1991; Odunaike *et al.,*2010; Akinmosin *et al.,* 2012; Anukwu *et al.,* 2014 and Olayinka *et al.,*2016 carried out since it was first discovered in 1901 by the Germans covers four states which are Edo, Ondo, Ogun and Lagos (Francis, 2016). Ako in 2003 reported that the oil sand belt extends eastward from Okitipupa (Ondo state) to Edo state's Siluko and Akotogbo districts, east of Ijebu-ode (Ogun state). These deposits of oil sands stretch in an east-west direction, measuring around 120 km in length and 4-6 km in width (Akinmosin *et al.,* 2012), with an estimated 30 to 42 billion barrels and about 3.6 billon barrels recoverable (Adegoke *et al.,*1991).

A few geophysical methods have been used to delineate the occurence of oil sand in Nigeria but with differing physical quantities. Akinmosin *et al.* (2011),(2012) and (2013) used electrical resistivity method to identify subsurface lithologies, ascertain depth of occurrence of bitumen and validate presence of oil sand in Imeri, Ogun state and Onikibiti, Ondo state. Akinmosin *et al.* in 2013 also studied the occurrence of oil sand at Ijebu-itele using electrical resistivity method to identify the nature and depth of occurrence of oil sand unit. They delineated the oil sand in the region as having high resistivity value of between 900 to > 1480 Ωm. Anukwu *et al.* (2014) and Adeyemi & Dairo (2015) on the other hand used 2-D electrical imaging technique together with induced polarization method and their results show high resistivity value and pronounced Induced polarization effect for oil sand at Imeri southwestern Nigeria. They concluded that electrical method is effective in characterizing oil sands.

Numerous hints about the origin and the environment of deposition of sedimentary rocks can be found in them. This information can be inferred from the shape and order of the rock layers, the grains of sediment, and the sedimentary structures, which include fossils, cross-beds, ripple lines, and mud cracks. The provenance of the material, the habitat in which it was deposited, and the origin of the sediment can all be determined by analysing the type of clast that is present. Finding and using critical minerals to forecast their dispersal pattern upon their return to the natural environment is made possible by an understanding of the distribution of

particle sizes and the heavy mineral assemblages found in sedimentary rocks, especially in the earth's crust (Pettijohn, 1975).

The presence of seepage is a good indicator of the availability of oil sand, and shallowness of its occurence. Adeyemi & Dairo (2015) and Iwueze & Alagbe (2021) reported low resistivity values for bituminous zones in Agbabu in contrast to previous research in the area by Amigun *et al*. (2012), Akimosin *et al*. (2012) and Opatola *et al*.(2022) to mention a few. Therefore, in this study our aim is to characterize the oil sand deposit by delineating zones of occurrence and evaluating the physical characteristics of the deposits to give probable provenance of the oil sand sediments .

**Geographic and Geologic Setting**

The study area is within Ondo state located in the southwestern part of Nigeria bordered in the North by Ekiti and Kogi states, while Edo state is to its East, Ogun and Osun to its west and Atlantic Ocean to its South. The state lies completely in the tropical region between longitudes 4°20" and 6°5" East of the Greenwich Meridian, 5°45" and 7°52" North of the Equator. Agbabu the study location falls within the southern part of the state and governed locally by Odigbo local government. The study area is within the Dahomey basin, an inland offshore coastal sedimentary basin in the Gulf of Guinea Oke *et al.*, 2016). According to Klemme (1975), the basin, which begins in Ghana's Volta-delta and ends on the western slopes of the Niger Delta in eastern Nigeria, spans a sizable chunk of the Gulf of Guinea's continental margin. This basin's oil sand is located in the eastern Dahomey basin's Nigerian section. (Adeyemi *et al.*, 2013).

The general stratigraphy of Dahomey Basin figure 1 has been studied by different people, Jones and Hockey 1964; Reyment, 1965; Adegoke (1969); Fayose, 1970; Omatsola & Adegoke (1981) among others, however, controversies still abound with respect to the different ages of the different formations.

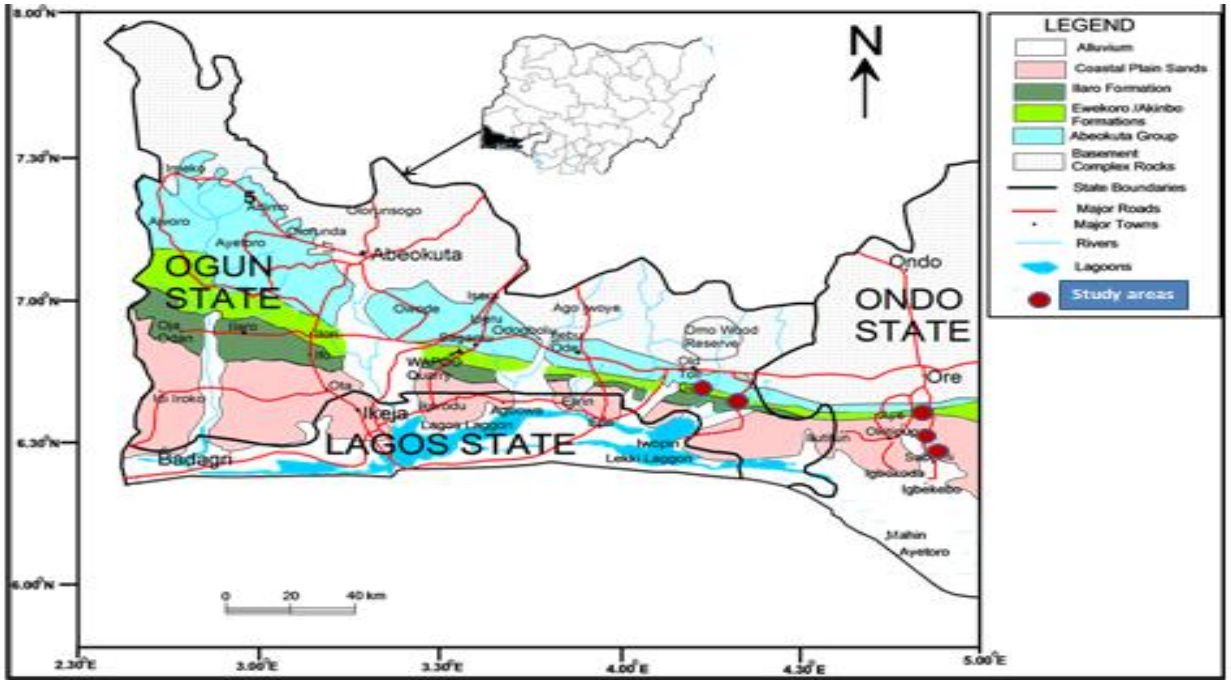


Figure 1: Geological Map of the Eastern Dahomey Basin (Source: Olabode and Muhammed 2016)

Jones and Hockey, 1964 classified the sedimentary basin into five major formations as reported by Akinmosin *et al. (2012)*. The stratigraphy of eastern margin of cretaceous to tertiary sedimentary sequence of the Dahomey Basin can therefore be divided into the following lithostratigraphic unit. The crystalline foundation complex is covered by the Ilaro, Ewekoro, Abeokuta, and Littoral deposits (Jones & Hockey, 1964), as well as the Coastal Plain sands. These formations range in age from Recent to Cretaceous. Ise formation, Afowo formation, and Araromi formation, among others, comprise the Abeokuta group; other formations include Akinbo and Ewekoro Formation, Oshosun Formation, and Ilaro Formation. Omatsola and Adegoke (1981), quoted by Akinmosin *et al*. (2013), presented a set of litho-statigraphic unit of formation as presented in table 1.

**Table 1: Classifications of formation within the study area**

| ERA | Jones and Hockey (1964) | | Omatsola and Adegoke (1980) | |
|---|---|---|---|---|
| | **Age** | **Formation** | **Age** | **Formation** |
| Quaternary | Recent | Alluvium | | |
| Tertiary | Pleistocene-Oligocene | Coastal Plain Sands | Pleistocene-Oligocene | Coastal Plain Sands |
| | Eocene | Ilaro | Eocene | Ilaro<br>Ososhun |
| | Paleocene | Ewekoro | Paleocene | Akinbo<br>Ewekoro |
| Late Cretaceous | Late Senonian | Abeokuta | Maastrichtian Neocomian | Araromi<br>Afowo<br>Ise |
| PRE – CAMBRIAN CRYSTALLINE BASEMENT | | | | |

## MATERIALS AND METHODS

The 2D electrical resistivity tomography data was obtained using the ABEM SAS1000 resistivity meter with ABEM LUND ES464 electrode selector. The measurements were done using 64 electrodes with 2.5m and 3m in which the electrode selector will automatically pick the set of four electrodes to be used at each measurement. The dipole–dipole array was employed for the 2D ERT. The general electrode configuration used in geophysics for subsurface resistivity measurements is such that two (pair) of electrode is used as the current (source) electrode and the other two used as the potential (receiver) electrodes. The dipole-dipole electrode configuration consists of two pairs of electrodes, the current and potential electrodes. Equal distances are maintained for both the current and potential electrodes which is denoted (a) and the distance between the current dipole and potential dipole is an integer multiple of 'a' (na) Figure 2. The advantages of dipole-dipole configuration are that it provides a data set which is a combination of profiling and sounding techniques, resulting in producing a detailed image. Another advantage is that it has high resolution and fast. The apparent resistivity was measured at the pseudosection point (Figure 2) using equation 1. Data was collected through seven traverses with individual length of 155 m because of restricted acquisition area. With profiles 1, 2, 3, and 4 orientated in a NE-SW direction and profiles 5, 6, and 7 in a NW-SE direction, the traverses were arranged to form a grid. (Figure 3).

$$\rho_a = \pi n(n+1)(n+2)a\frac{\Delta V}{I} \quad (1)$$

Where $\rho_a$ is the apparent resistivity, n is the integer and a is the distance between the dipole electrodes.
$\Delta V$ is the potential difference, and I is the current.

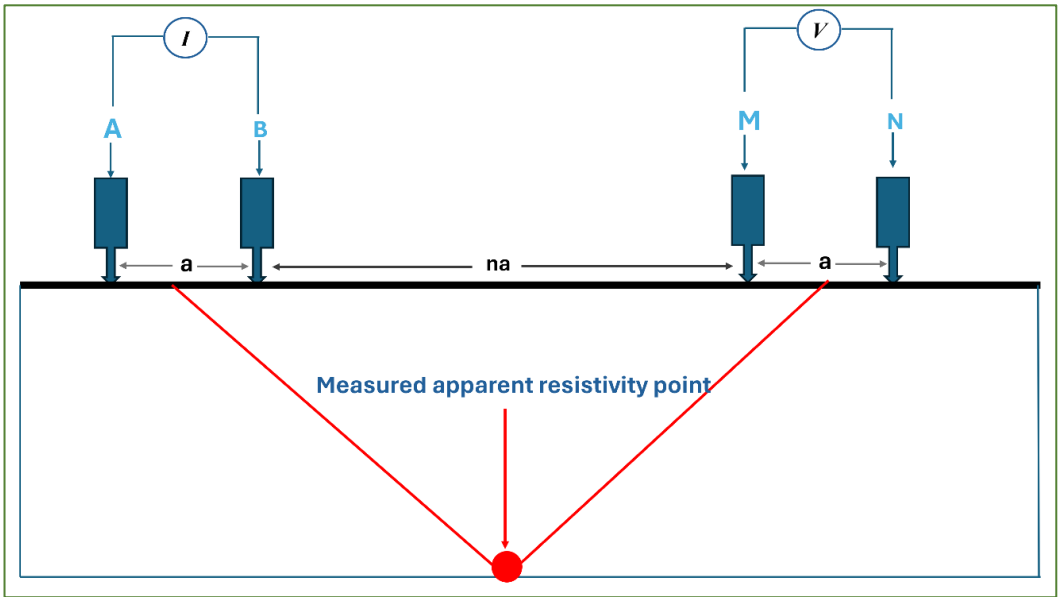


Figure 2: Dipole-dipole configuration showing the electrodes and apparent resistivity data point (Coker *et al*., 2017) (Coker, Odunaike, & Adekoya, 2017)

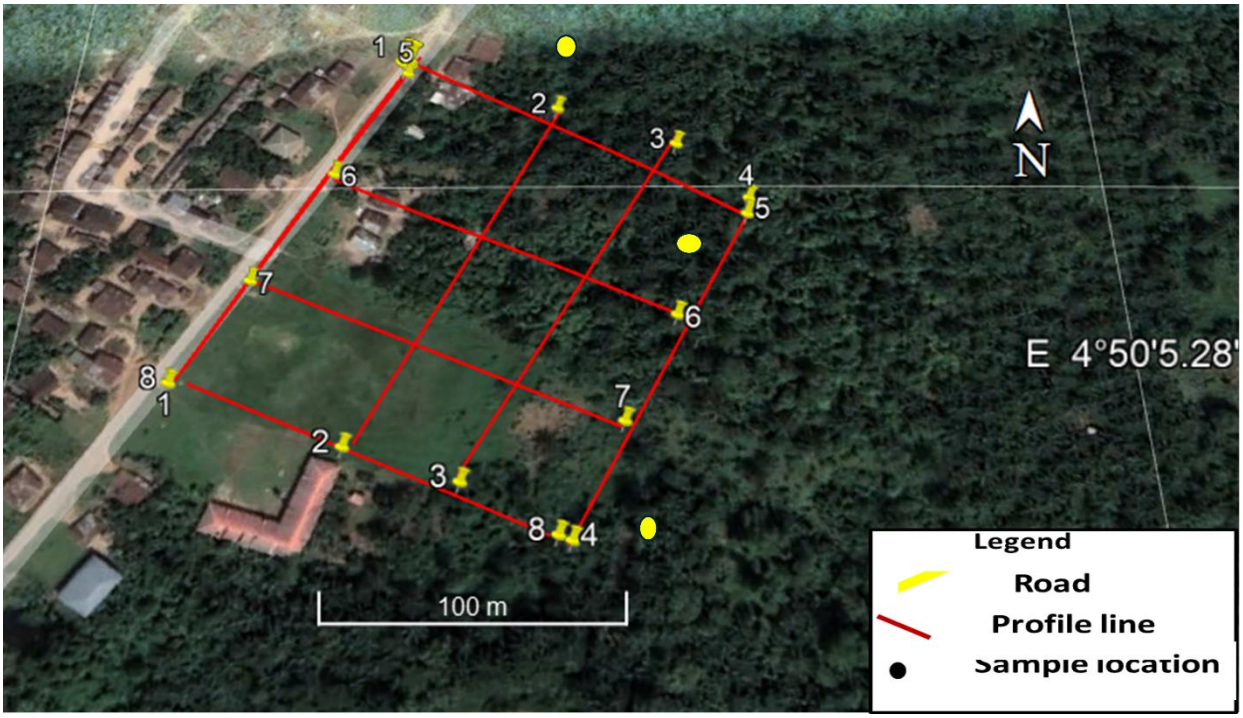


Figure 3: Base mapof the study area showing the orientation of the profle lines

This allowed for proper 3D imaging and oil sand delineation. The RES2DINV software was used to analyze the collected data. To create a better forward model, we applied the conjugate gradient forward modeling technique along with the finite element method. Following that, due to the robustness and density of the gathered resistivity data, inversion was carried out using the smooth model-based inversion method and the quasi-Newton optimization technique rather than Gauss Newton's least square approximation routine for quick computation times as well as to arrive at satisfactory and geologically meaningful 2D resistivity distributions that will be used for the 3D image.

A total of three samples were collected at three different points in the study area. Handheld GPS was used to take the coordinates and elevation above sea level at sampling points. To avoid sample contamination, precautions were taken during the sample collection process hence the weathered surface of the outcrop was chipped away to expose fresh surface after which a hand trowel was used to take the sample. The oil sand samples were put in sample bags and labelled accordingly before being taken to the laboratory for processing.

## RESULTS AND DISCUSSION

### Electrical resistivity tomography results

ERT profile 1: The first dominant layer resistivity value as evident in ERT 1 psuedosection (figure 4a) ranges from 50-950 Ωm and terminates at a depth of 5 m along the NE-SW direction. The ERT terminates in the second layer which is a high resistivity formation inferred to be oil sand with resistivity value above 1900 Ωm. The depth of occurrence of the oil sand on this profile starts from 1m where it is close to the surface at around line position 160 m. The depth of occurrence is not uniform along the profile.

ERT profile 2: ERT 2 was acquired parallel at a distance of approximately 50m away from ERT 1 along the NE-SW direction. ERT 2 is a 158 m long profile revealing three principal geoelectric layers (Figure 4b). The resistivity value of the uppermost geoelectric unit in the profile ranges from 40 to 750 Ω m, while its thickness varies from 1 to 3 m. Laterally, this geoelectric layer transforms into bitumen-impregnated sand with resistivity more than 2000 Ωm. This layer is seen to overlie another layer as evident in the change in resistivity value of less than 900 Ωm around line position 20-30 m and 60-80 m along the profile and at depth of 11m. The third layer is inferred to be sand interbedded with clay.

ERT profile 3: ERT 3 is 158 m long, with an imaging depth of up to ~14 m and in the NE-SW direction. In this ERT 3, the variation in resistivity is seen to range from 40 Ω m to 62,599 Ω m as shown in Figure 4c. The topmost layer has resistivity value between 40 Ω m to 450 Ω m and a thickness range of 1m to 3m and it starts from line position 40 m to the end of the profile. The second depicted geoelectric layer has resistivity value greater than 3500 Ω m with thickness ranging from 11 m to 13m. This second layer is inferred to be oil sand

because of its very high resistivity value, and it is seen to be very close to the surface around the Northeastern part of the profile.

ERT profile line four: Figure 4d shows the geoelectric section of profile line four. This 2-D resistivity section along profile line 4 reveals three geo-electric layers. The first layer has resistivity ranging from 10-650 Ωm, with a thickness range between 1-3 m and inferred as the topsoil, the second layer has resistivity value from 2000 Ωm to over $10^5$ Ωm with thickness ranging from 8-11m. The underlying layer can only be seen in this ERT around line position 60 -70 m and from 80-100 m at a depth of approximately 9 m form the surface. The resistivity of this third layer ranges from 270-850 Ωm.

ERT profile line five: The first dominant layer on ERT 5 oriented along the NW- SE direction as observed in Figure 5a has resistivity value ranging from 10-250 Ωm and terminates at a depth range of 1- 5 m. The second layer is a high resistivity formation of value ranging from 1500 - > $10^5$ Ωm and thickness of 1-12 m and it is inferred to be oil sand formation. The underlying third layer which is the last layer is a low resistivity formation when compared to the overlying formation inferred to be sandy clay with resistivity value from 250 -500 Ωm.

ERT profile line six: Figure 5b shows ERT for profile line six which was acquired parallel and at a distance of approximately 50m away from ERT 5 along the NW-SE direction. It was observed that there are two dominant layers identified on this profile terminating at a depth of approximately 13.5 m; top soil with a resistivity range of 10 -250 Ωm , and oil sand with a resistivity value > 2500Ωm.

ERT profile line 7: In this ERT 7, the variation in resistivity is seen to range from from 10 Ωm to over 10,000 Ωm as shown in Figure 5c. Two distinct geoelectric unit can be observed in this profile. The topmost layer has resistivity value between 40 Ωm to 650 Ω m and a thickness range of 1m to 3.5m. The second layer is inferred to be oil sand because of its very high resistivity value ranging between 1500 and > 60,000 Ωm. This profile terminates within the oil sand formation.

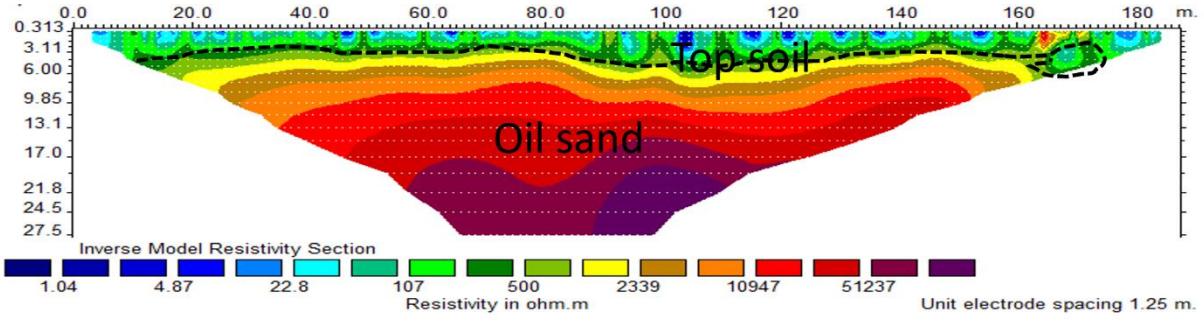


a) Electrical resistivity tomography of profile one

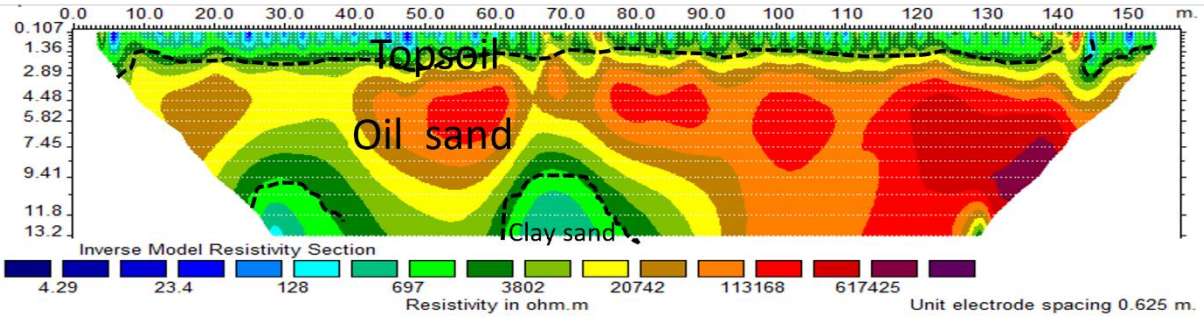


b) Electrical resistivity tomography of profile two

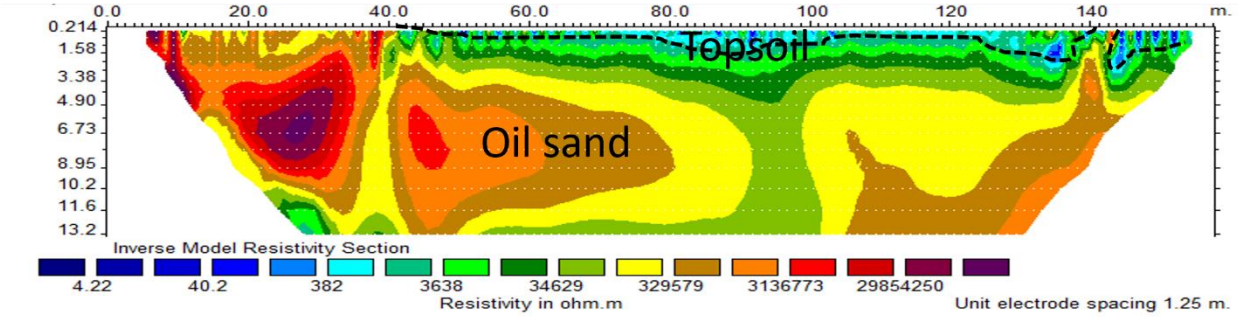


c) Electrical Resistivity tomography for profile three

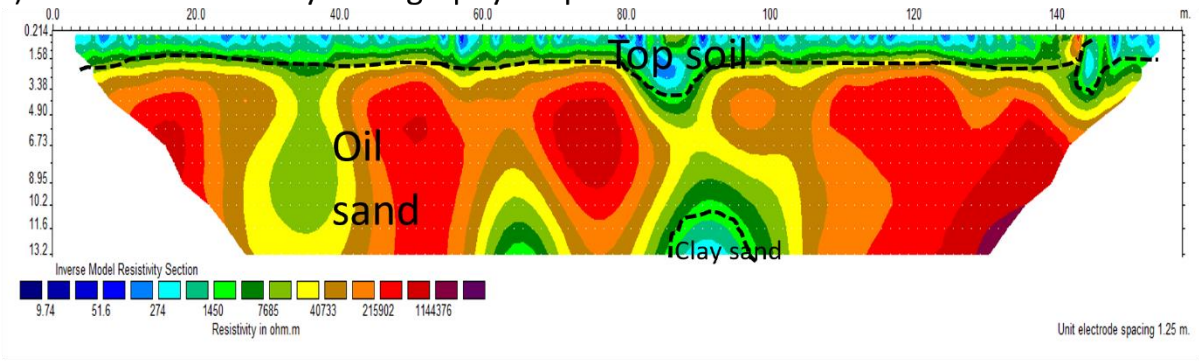


d) Electrical resistivity tomography for profile four

Figure 4a-d: Electrical resistivity tomography section for profile 1-4.

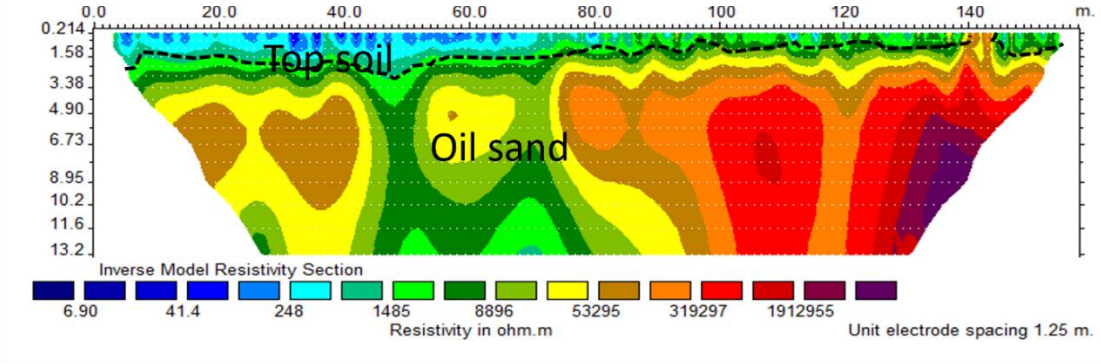


a) Electrical resistivity tomography of profile five

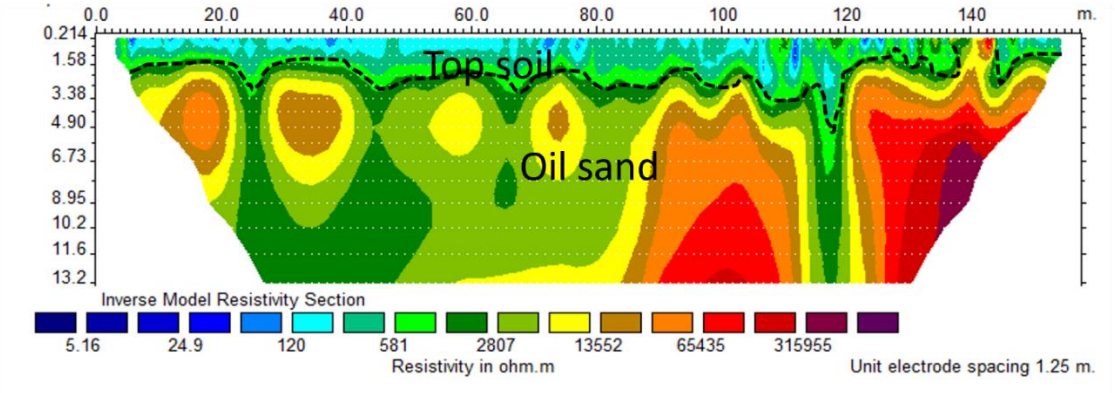


b) Electrical resistivity tomography of profile six

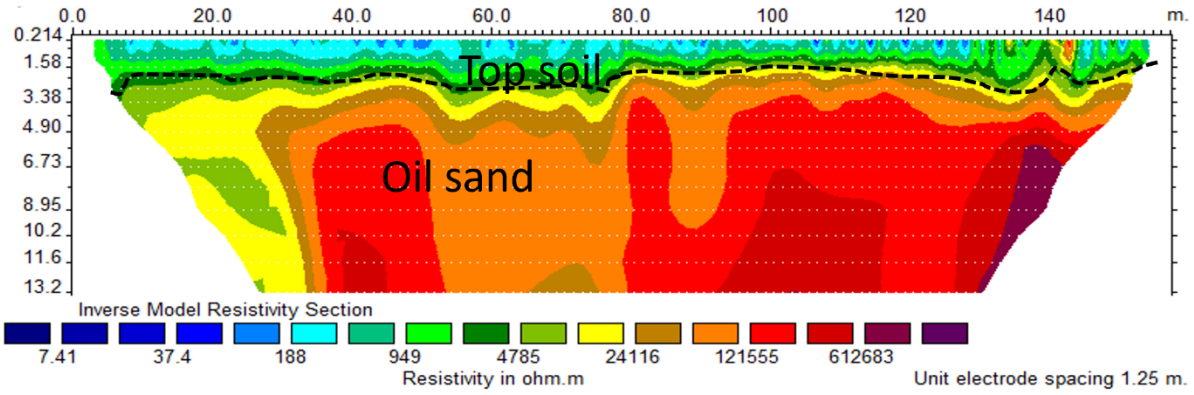


c) Electrical resistivity tomography of profile seven

Figure 5a-c: Electrical resistivity tomography section for profile 5-7

**Result of the 3D ERT of the study area**

The inverted 3-D model reveals the presence of three geoelectric layers, topsoil, oil sand and clayey sand, with resistivity value range of 150 -650 Ωm, $>10^5$ Ωm and 550-1500 Ωm respectively.

The 3-D model is sliced along the z-axis which gives a clear view of the vertical variation in relation to depth at 0.88 m, 1.88 m, 3.04 m, 4.37 m, 5.90 m, 7.66 m, 9.68 m, 12.0 m, and 14.7 m to ascertain the lithological unit's variation.

Figure 6b shows the topsoil at depth of 0.88m, reveal the presence of the oil sand in the northern part of the area and slightly the around the southeastern and southern part of the study area while other part is mostly topsoil. The next slice shows the lithologic unit at 1.88 m revealing the extension of the oil sand and part of the topsoil being replaced by the oil sand. Figure 6d shows the lithologic unit at 3.04 m revealing the disappearance of the topsoil completely around the northeastern and southeastern part of the study area and replaced by the oil sand. Figure 6e shows the layer at 4.37 m where little or no topsoil (blue through lemon green) can be seen in this plane and the oil sand is seen spreading.

Figure 6f, 6g, and 6h shows the soil has completely disappeared and the oil sand is more visible in the area. Figure 6i and 6j shows the re-emergence of another layer around the western part of the study area with a differing resistivity value of 550 – 1200 Ωm inferred to be clayey sand.

**Results of the Sedimentological analysis**

This section presents the result of granulometric analysis used in making sedimentological characterization. The result and interpretation are done in terms of grain sizes, sorting, skewness and kurtosis.

**Grain Size**

The raw data obtained from the sieving exercises were input in the software for processing to obtain the grading curves and textural parameters and statistical variables such as the mean, standard deviation (sorting), skewness and kurtosis. Table 2 presents the summary of the statistical parameters and their respective interpretations deduced from the cumulative frequency curve and histogram pictorial views of each sample as depicted in Figures 7a-f.

The mean values obtained from logarithmic scale of cumulative frequency curves (Figure 7a-f.) of samples from the location were calculated in accordance with Folk and Wards' (1957) and Ikhane *et al.* (2013) research and the value range from 1.07 (Ondo-3) through 1.2 (Ondo-2) and 1.38 for Ondo-1 samples which are all classified into medium sand grade. The sorting values for the Ondo-1, 2, and 3 samples vary from 1.207 (Ondo-3) through 1.23 (Ondo-1) to 1.342 for Ondo-2 samples. The sediments were all classified into moderately sorted class after (Blott & Pye, 2001).

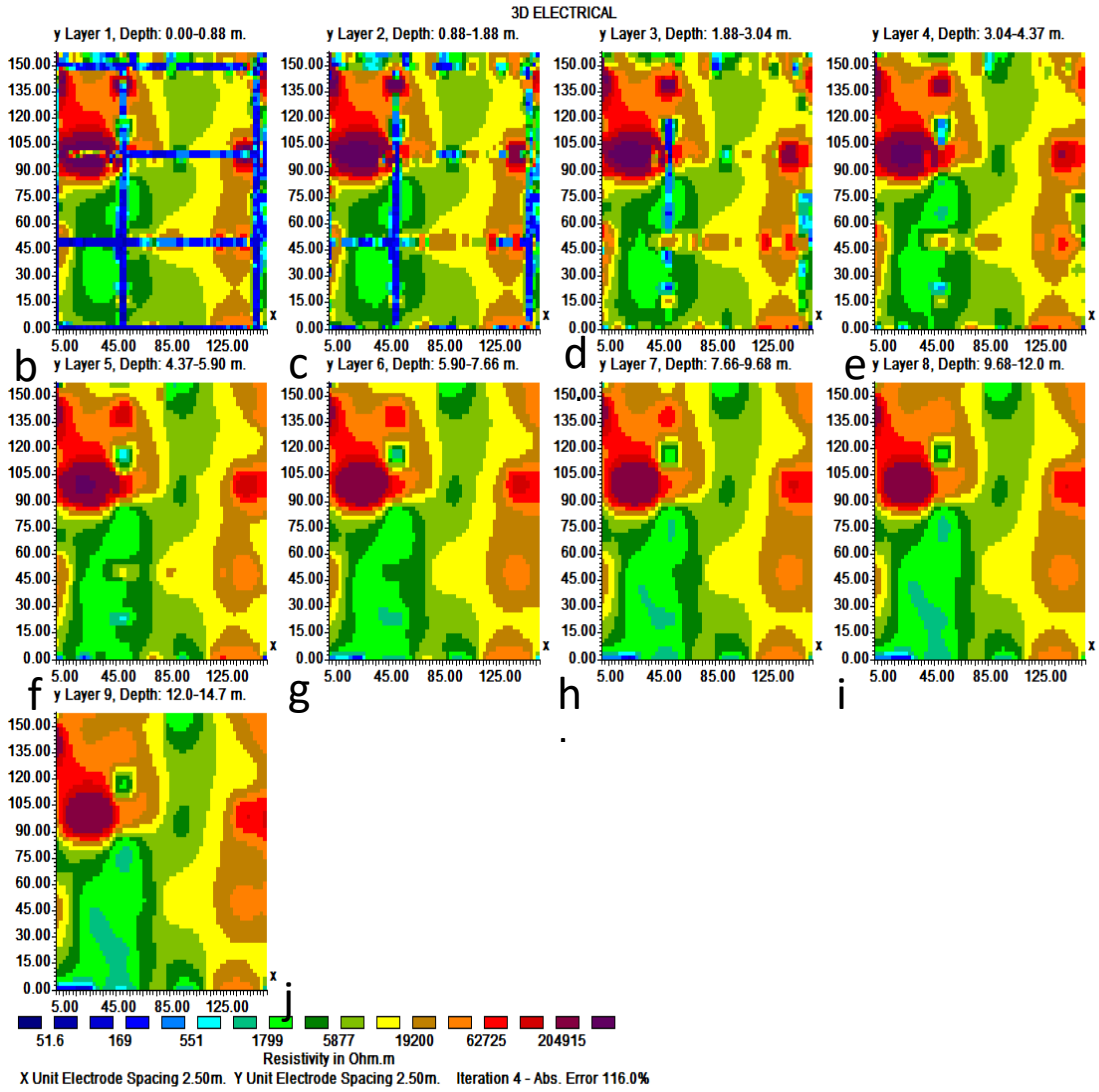


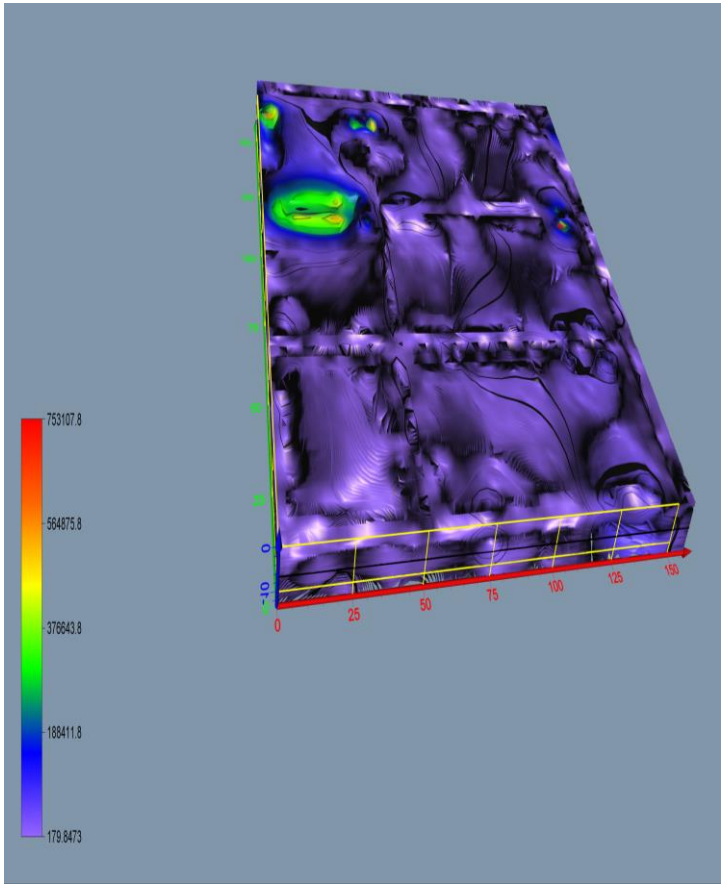


a) 3-D model of the study areaa) Electrical resistivity tomography of profile one

Figure 6: 3D-model and 3-D depth slice of the study area

Skewness is a measurement used to infer the symmetry and consistency of sample particle size distribution, which helps identify the dispersion status of sediments. The results are classified using the classification of Folk, 1980, where the skewness exhibited by the Ondo-1, 2, and 3 samples is
presented in Table 2. The skewness values are nearly symmetrical for Ondo-1 and Ondo-3 samples, while the Ondo-2 sample is defined by severely fine skewed. The nearly symmetrically skewed samples suggest having even distribution of the grain sizes at both head and tail of the transportation of the sediments. However, Ondo-2 sample is characterized by severely fine skewed, indicative of having a relatively fine grains in the assemblage than other sand size classes.

**Table 2: Summary of weight retained in sieve sizes for all samples**

| Sieve (mm) | Phi (Ø) | Ondo-1 | Ondo-2 | Ondo-3 |
|---|---|---|---|---|
| 2.00 | -1.00 | 2.84 | 2.45 | 3.90 |
| 1.18 | -0.25 | 6.80 | 6.24 | 9.05 |
| 0.85 | 2.5 | 1.11 | 9.46 | 12.45 |
| 0.60 | 0.75 | 11.60 | 9.96 | 11.79 |
| 0.425 | 1.25 | 22.15 | 16.15 | 18.80 |
| 0.30 | 1.75 | 21.54 | 15.18 | 18.30 |
| 0.25 | 2.0 | 10.50 | 8.32 | 7.30 |
| 0.15 | 2.75 | 11.94 | 17.74 | 9.28 |
| 0.10 | 3.25 | 10.45 | 7.55 | 2.50 |
| 0.075 | 3.75 | 0.32 | 2.20 | 1.77 |
| 0.063 | 4.0 | 0.30 | 3.80 | 4.30 |
| Pan | 5.0 | 0.40 | 0.80 | 0.20 |

**Table 3: Summary of statistical grain size parameters and their interpretation**

| Sample | Ondo-1 | Ondo-2 | Ondo-3 |
|---|---|---|---|
| **MEAN** | 1.38 | 1.2 | 1.07 |
| | Medium sand | Medium sand | Medium sand |
| **SORTING** | 1.23 | 1.342 | 1.207 |
| | Moderately sorted | Moderately sorted | Moderately sorted |
| **SKEWNESS** | 0.042 | 0.32 | 0.04 |
| | Nearly symmetrical | Severely fine skewed | Nearly symmetrical |
| **KURTOSIS** | 1.32 | 4.48 | 1.15 |
| | Leptokurtic | Mesokurtic | Leptokurtic |

The qualitative measurement of sediments that have been sorted elsewhere in a high energy environment before being transported and altered by a different type of environment is represented by the graphic kurtosis as presented by Folk and Ward (1957) and Ikhane *et al.* (2013). The kurtosis of the parameter calculated for the Ondo-1, and 3 wells sandstones indicated leptokurtic, which suggests a unimodal source; while the mesokurtic attributed to Ondo-2 sandstone sample was indicative of bimodal source of sediment supply (Table 2). In terms of reservoir properties, the Ondo-1, 2, and 3 samples are characterized by relatively good reservoir quality. All these values are indicative of the peak of the frequency curve and dominance of a particular class size.

The textural group interpretation shows that the three samples belong to a sand class (Table 4). This agrees with the gravel-sand-mud and sand-silt-clay ternary diagrams (Figure 8) where all the samples plotted in the sand corner.

**Table 4: Summary of sample type, textural group and sediment names**

| Sample no. | Sample type | Textural group | Sediment name |
|---|---|---|---|
| Ondo- 1 | Unimodal, Moderately sorted | Sand | Medium sand |
| Ondo- 2 | Bimodal, Moderately Sorted | Sand | Medium sand |
| Ondo- 3 | Unimodal, Moderately Sorted | Sand | Medium sand |

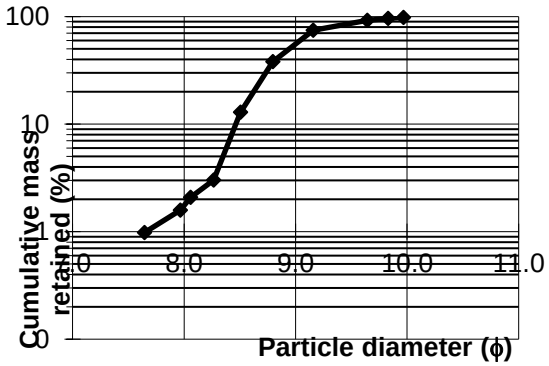


(a) Cumulative % vs Particle size (phi), Ondo-1

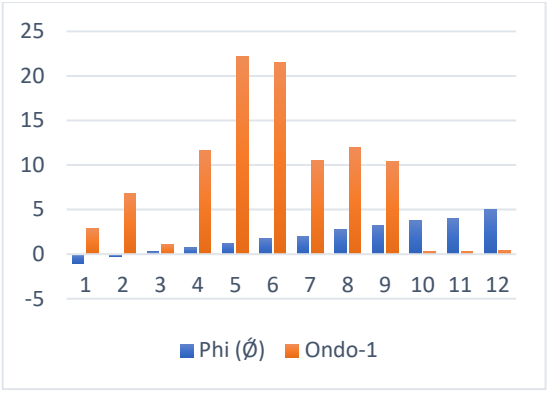


(b) Histogram of particle size distribution of Ondo-1

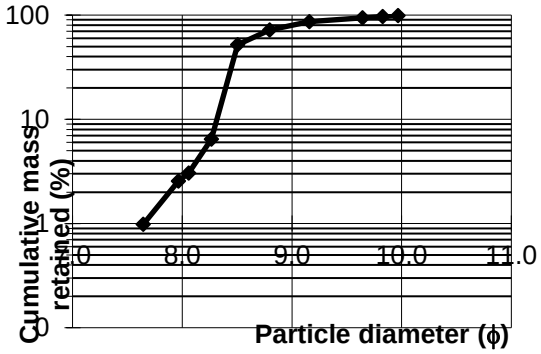


(c) Cumulative % vs Particle size (phi), Ondo-2

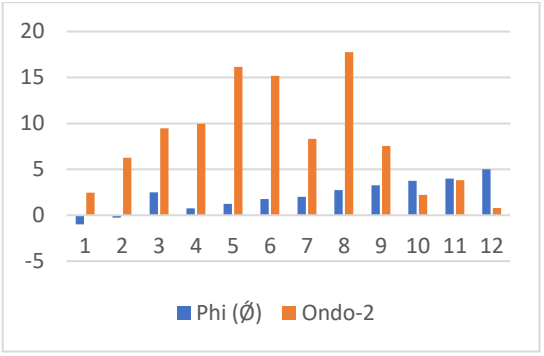


(d) Histogram of particle size distribution of Ondo-2

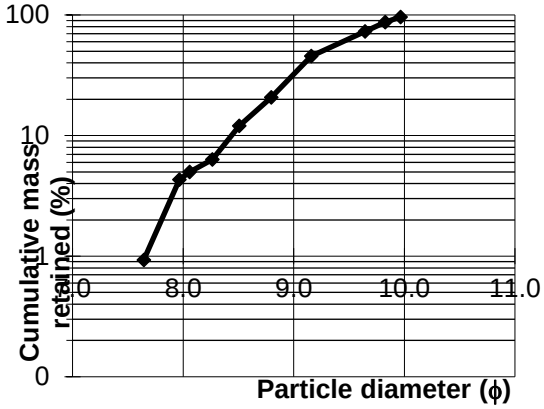


(e) Cumulative % vs Particle size (phi), Ondo-3

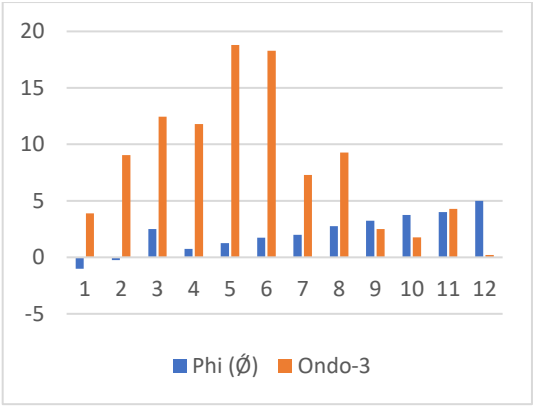


(f) Histogram of particle size distribution of Ondo-3

Figure 7: Cumulative frequency curve and Histogram of Ondo samples

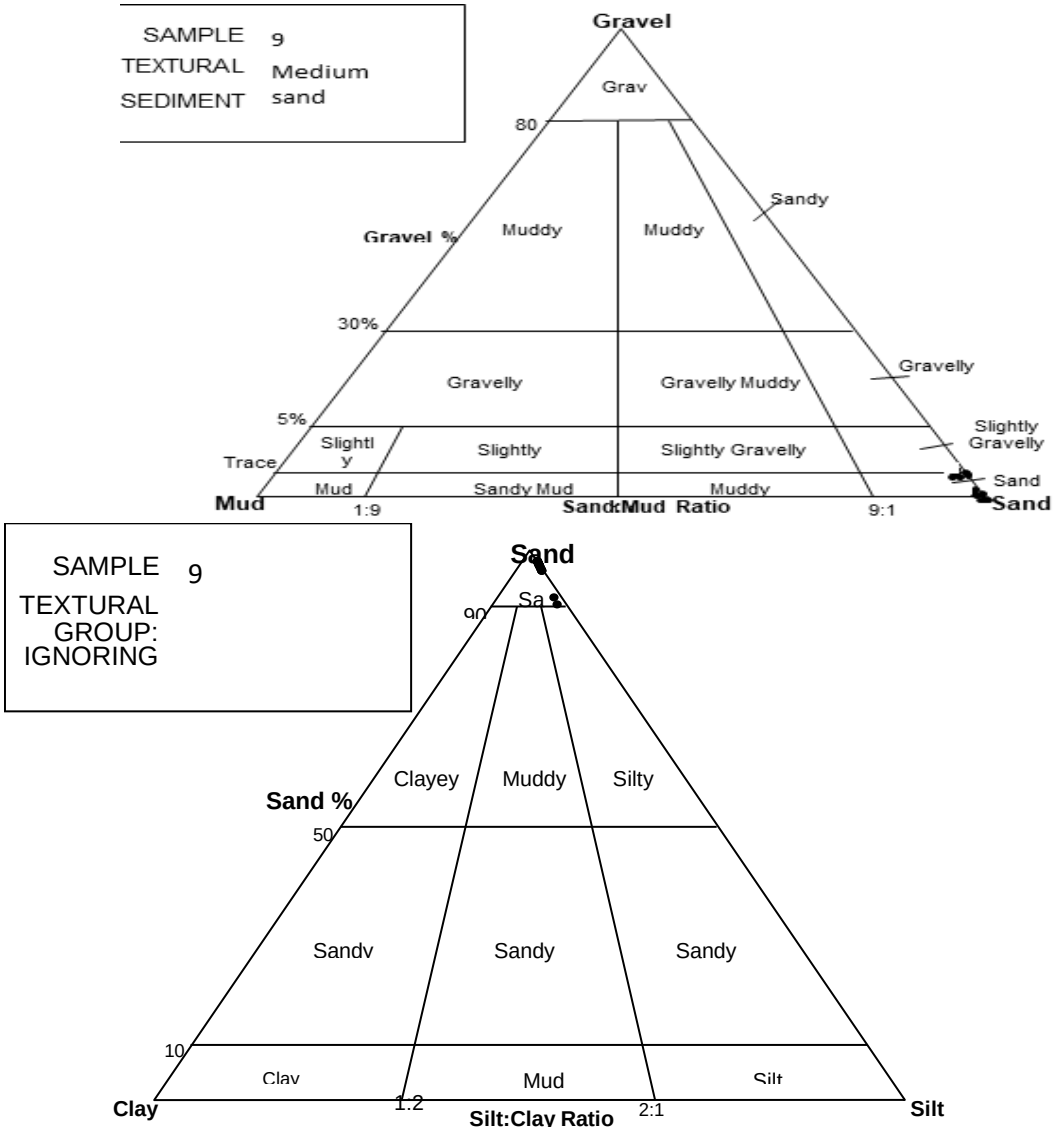


Figure 8: The gravel-sand-mud and sand-silt-clay ternary diagram of the analysed samples

## CONCLUSION

In this research work, 2-D and 3-D electrical resistivity tomography and sedimentological analysis were done to characterize oil sand in the study area. The 2-D ERT aided in delineating the geoelectric units of the subsurface including oil sand occurrence with resistivity value ranging from 2000 Ωm to over 250,000 Ωm and thickness ranging from 3m to 14 m across the study area. The delineated geoelectric unit include topsoil, oil sand and clayey sand. The presented subsurface geo-resistivity 3-D model shows how the ground resistivity value varies across the field. This survey has given the lithological successions of the subsurface layering at the study area. The resistivity value of oil sand in this area has high resistivity value as reported by Amigun *et al.*, 2012 and Akinmosin *et al* 2012 and Opatola 2022 and contradicts the reports of low resistivity reports of Adeyemi & Dairo, (2015) and Iwueze & Alagbe, (2021) owing to the fact that when the porespaces of sandstones is completely filled with oil or gas, which are non-conducting, the rocks constituted with sand sdiments having high to moderate porosities can have very high resistivities. The sedimentological characterization reveals that the oil sand of the study is of the medium sand group, moderately sorted thought to be from both single source (unimodal) and two sources (bimodal).

This research work has provided a clear insight of the gradual and exponential, lateral and horizontal variation in subsurface material's geophysical and geological properties and its implication in re-writing the history of the earth materials. However, other approach which entails other near surface geophysical methods like GPR and seismic refraction methods as well as further sedimentological analysis is recommended in the area.

**REFERENCES**

Adegoke, O., Omatsola, M., & Coker, J. (1991). The Geology of the Nigerian tar sands. *5th Unitar International conference on Heavy crude an Tar sand AOSTRA Technical report.*

Adeyemi, G., & Dairo, V. A. (2015). Subsurface Models of Abitumen-Rich Area near Ode-Irele, Southwestern Nigeria. *IOSR Journal of Applied Geology and Geophysics (IOSR-JAGG),, 3*(14), 13-19.

Adeyemi, G., Akinmosin, A., Aladesanmi, A., & Badmus, G. (2013). Geophysical and Sedimentological Characterization of a Tar Sand Rich Area in South-western Nigeria. . *Journal of Environment and Earth Science, 3*(14), 71-83.

Akinmosin, A. A., Omosanya, K., Ikhane, P., Mosuro, G., & Goodluck, I. (2012). Characterization of a bitumen seepage in Eastern Dahomey Basin. *Advances in Applied Science Research, 3*(4), 2078-2089.

Akinmosin, A., Omosanya, K. O., Ariyo, S. O., Folorunsho, A. F., & Aiyeola, S. O. (2011). Structural Control of Bitumen seepages in Imeri, Southwestern Nigeria. *International Journal of Basic & Applied Sciences IJBAS-IJENS, 11*(1), 61-67.

Akinmosin, A., Omosanya, K., & Ige, T. (2013). The Occurrence of Tar Sands at Ijebu-Itele, Eastern Dahomey Basin, SW, Nigeria. *ARPN Journal of Science and Technology, 3*(1), 98-105.

Ako, B. D. (2003). Exploration strategies for Bitumen Saturated Sands in Nigeria: Prospects for investments in mineral resources of southwestern Nigeria. In Elueze, A.A 2008,. . *Nigerian Mining and Geosciences Society,*, 61-66.

Anukwu, G. C., Odunaike, R. K., & Fasunwon, O. (2014). Oil sand exploration using 2-D electrical imaging technique. . *Journal of Natural Sciences Research,, 4*(4), 68-73.

Francis, I. N. (2016). Prospects of Tar Sand in Nigeria Energy Mix. *The International Journal of Engineering and Sciences, , 5*(12), 84-89.

Ikhane, P., Akintola, A., & Osiniwo, A. (2013). Heavy Mineral Characteristics and grain size distribution of the siliciclastic sediments in Ijebu-Omu, Iloti, Itele and Ijebu-ife study areas of eastern Dahoey basin southwestern Nigeria. *Research Journal of Earth and Planetary Sciences, 3*(1), 13-37.

Iwueze, E. S., & Alagbe, O. (2021). Application of Electrical Resistivity Techniques forMapping Bitumen Saturated Zones and Its Geologic Implication over Agbagbu, Southwestern Nigeria. . *Earth Sciences,, 10*(6), 332-345.

Jones, H., & Hockey, R. (1964). The Geology of Part of South-western Nigeria: Explanation of 1:250,000 sheets Nos. 59 and 68. *Geological Survey of Nigeria*.

Jones, H., & Hockey, R. (1964). The Geology of Part of South-western Nigeria: Explanation of 1:250,000 sheets Nos. 59 and 68. *Geological Survey of Nigeria.*

Klemme, H. (1975). Geothermal Gradients,Heatflow and Hydrocarbon Recovery. . *Petroleum and Global Tectonics.*

Odunaike, R. K., Laoye, J. A., Fasunwon, O. O., Ijeoma, G. C., & Akinyemi, L. P. (2010). Geophysical mapping of the occurrence of shallow oil sands in Idiopopo at Okitipupa area, South-western Nigeria. *African Journal of Environmental Science and Technology, 4*(1), 34-44.

Oke, S., Vermeulen, D., & Gomo, M. (2016). Aquifer vulnerability assessment of the Dahomey Basin using the RTt method. *Environ Earth Science.*

Olayinka, A., Oladunjoye, M., & Korodele, A. (2016). 2-D Electrical Resistivity Imaging of Tar sands Seepages in Ilubirin, Southwestern Nigeria. *International Journal of Advancements in Research & Technology,, 5*(11), 18-28.

Omatsola, M., & Adegoke, O. (1981). Tectonic evolution and Cretaceous stratigraphy of theDahomey basinin Adekeye et al (eds.): Hydrocarbon Potential Assessment of the Upper Cretaceous-Lower Paleogene-Neogene Sequence in the Dahomey Basin Southwest. *Nigeria Journal Mining and, , 18*(1), 130-137.

Opatola, A., Obafemi, S., Bankole, S. I., Akinwale, R. P., & Alli, S. A. (2022). Geoelectrical resistivity mapping and characterization of bituminous sands at some parts of Eastern Dahomey Basin, SW Nigeria. *Egyptian Journal of Petroleum, 31*, 33-38.

Pettijohn, F. J. (1975). Sedimentary rocks. New York: Harper & Row.

Reyment, R. A. (1965). Aspects of the Geology of Nigeria: the stratigraphy of the cretaceous and cenozoic deposits.